

EXPERIMENTAL STUDY OF CONDENSATION OF BINARY VAPORS ON A SHORT HORIZONTAL TUBE

TAKSHIRO MAMYODA, HITOSHI KOSUGE AND
KOICHI ASANO

*Department of Chemical Engineering, Tokyo Institute of Technology,
12-1, Ookayama-2, Meguro-ku, Tokyo, 152*

Key Words: Condensation, Heat transfer, Mass transfer, Binary vapor mixture, Simulation, High mass flux, Horizontal tube

Experiments on the condensation of binary vapor mixtures of methanol-steam and acetone-ethanol systems on a short horizontal tube were made for a wide range of vapor flow rates and concentrations. The observed vapor phase sensible heat and diffusion fluxes showed good agreement with the authors' previous numerical correlation for heat and mass transfer on a cylinder with high mass flux effect.

The effect of vapor flow rates and cooling water temperatures on partial condensation, where the concentration of condensate is lower than that of vapor free stream, was discussed. A new method for predicting the concentrations of condensate of binary vapor mixtures on a short horizontal tube was proposed, and compared with the experimental data under total and partial condensation.

Introduction

Condensation of binary vapor mixture is an important problem for design of total and partial condensers in distillation. Although many theoretical (Asano and Matsuda, 1985, Denny and Jusionis, 1972, Fujii and Koyama, 1985, Fujii *et al.*, 1989, Sykes and Marchello, 1970) and experimental (Asano and Matsuda, 1985, Bandrowski and Bryczkowski, 1975, Pressburg and Todd, 1957, Sykes and Marchello, 1970) investigations were made for the condensation of binary vapor mixtures, there still remain some uncertainties regarding the surface temperatures and concentrations of condensate under partial condensation and the effect of operating conditions on the transition from total to partial condensation.

In our previous paper (Mamyoda and Asano, 1994), heat and mass transfer in condensation of vapors with noncondensable gas on a short horizontal tube was experimentally examined. The result showed that the vapor phase sensible heat and diffusion fluxes agreed well with our previous numerical analysis (Mamyoda and Asano, 1993). The purpose of the present study is to make an experimental approach to condensation of binary vapor mixtures on a short horizontal tube, and to compare the experimental data with the results of our previous numerical analysis.

1. Experimental Apparatus and Procedures

1.1 Apparatus

Figure 1 shows a schematic diagram of the experimental apparatus. The test condenser was a 40 mm long, 9.0 mm O.D. and 0.5 mm thick copper tube. For the measurements of wall temperature, two 0.5 mm O.D.

sheathed Chromel-Alumel thermocouples were soldered on the surface of the condensing tube 2 mm from both ends of the condensing tube at angles of $\pi/2$ from the forward stagnation point. Near the condensing tube on the equatorial plane of the tube cross section, a 0.25 mm O.D. sheathed Chromel-Alumel thermocouple was mounted by a traversing mechanism for measurements of the vapor phase temperature profiles. Downstream of the condensing tube, a condensate collector was installed and connected to a measuring cylinder. Details of the test section are shown in elsewhere (Mamyoda and Asano, 1994).

1.2 Measurements

Surface temperatures of the condensate and vapor phase sensible heat fluxes: The observed vapor phase temperatures near the condensing tube (6-8 points) at $\theta = \pi/2$ were smoothed by use of the least square method with a quadratic equation:

$$T_{G, \theta = \pi/2} = a(r - R)^2 + b(r - R) + c \quad (1)$$

The surface temperatures of the condensate, $T_s, \theta = \pi/2$, were estimated from the smoothed vapor phase temperature profiles by an extrapolation method with an accuracy of ± 1 K. The vapor phase local sensible heat fluxes at $\theta = \pi/2$ were evaluated from the smoothed temperature profiles at the surface by numerical differentiation with respect to radial distance.

Flow rates and concentrations of the condensate and the vapor: The flow rates of the condensate over the condensing tube were determined from the amount of the liquid received by a measuring cylinder for the test section for a given time interval. The flow rates of the vapor were determined from the amount of liquid from total condenser added with the one from the test section by a

* Received September 1, 1994. Correspondence concerning this article should be addressed to K. Asano.

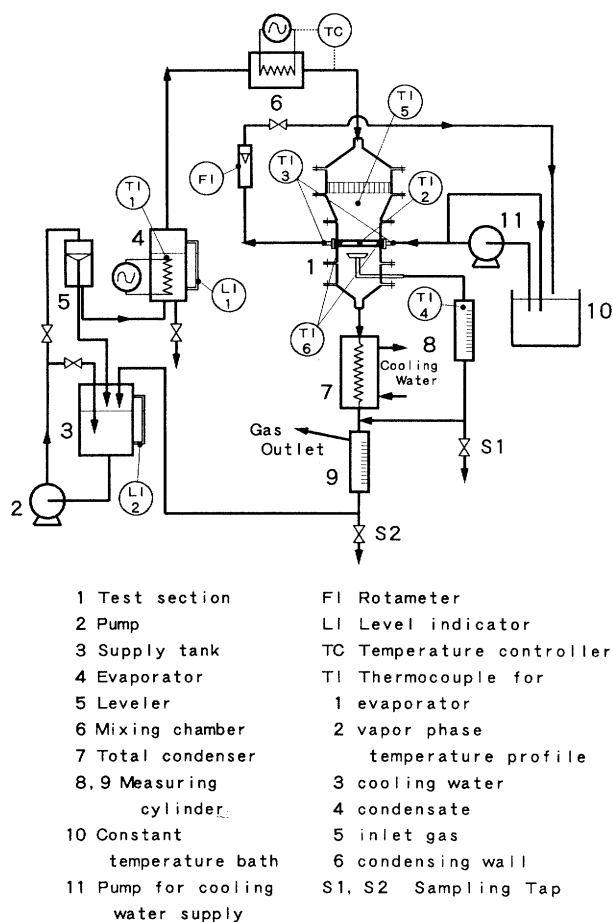


Fig. 1 Schematic diagram of experimental apparatus

similar way. The concentrations of the condensate and the vapor were determined from the liquid samples from the measuring cylinder for the test section and the one from total condenser by a gas chromatograph with an accuracy of 0.3 mol%.

Vapor phase mass and diffusion fluxes: The vapor phase average mass fluxes for each component over the surface of the condensing tube, \bar{N}_A , \bar{N}_B , were obtained from the flow rates and concentrations of the condensate. The diffusion fluxes for each component, \bar{J}_A , \bar{J}_B , were obtained from the mass fluxes by using the following equation:

$$\bar{J}_A = \bar{N}_A - (\bar{N}_A + \bar{N}_B) \omega_{As} \quad (2.a)$$

$$\bar{J}_B = \bar{N}_B - (\bar{N}_A + \bar{N}_B) (1 - \omega_{As}) \quad (2.b)$$

where ω_{As} is the equilibrium vapor mass fraction of the more volatile component at surface temperatures of the condensate.

Validity of the measurements: In order to confirm the validity of the measurements, condensation of pure methanol vapor was carried out for a wide range of cooling water temperatures. The observed condensation heat transfer coefficients agreed with Nusselt's model within 15% (Mamyoda and Asano, 1994).

1.3 Vapor-liquid equilibria and physical properties

Vapor-liquid equilibria of the methanol-steam and the acetone-ethanol system were estimated from the vapor pres-

Table 1 Experimental conditions

System	Re_G	y_∞	T_{Cwin}
Methanol-Steam	39-380	0.30-0.85	278-320
Acetone-Ethanol	122-370	0.49-0.53	279-284

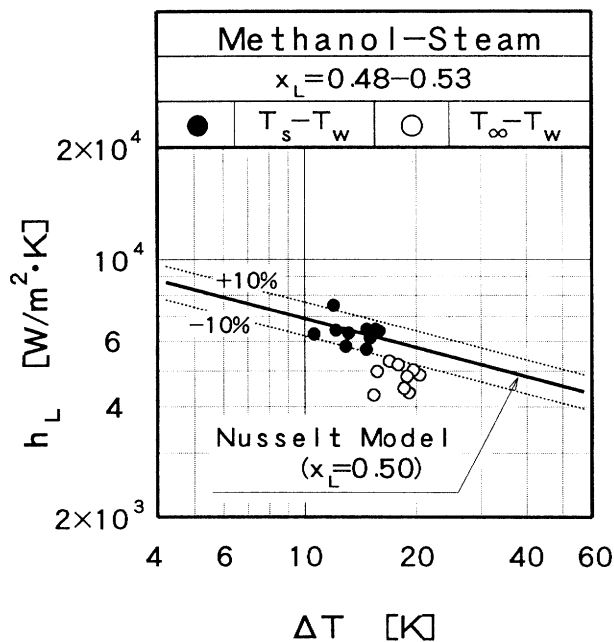


Fig. 2 Condensation heat transfer coefficient; a comparison with Nusselt's model

ures of pure components by Antoine's equation and the liquid phase activity coefficients by Wilson's equation.

The physical properties of the vapor mixtures were evaluated at their vapor phase concentrations and temperatures of the condensate at $\theta = \pi/2$, $T_{s, \theta = \pi/2}$. The viscosities and the thermal conductivities of the vapor mixtures were estimated by Wilke's method. The viscosities of the pure vapors were estimated by Hirschfelder's method, and the thermal conductivities by Eucken's method. The binary diffusion coefficients of the vapor were estimated by Hirschfelder's method.

Physical properties of the condensate were evaluated at their reference temperatures defined by (Minkowycz and Sparrow, 1966):

$$T_{ref} = T_w + (T_s - T_w) / 3 \quad (3)$$

1.4 Ranges of variables

Condensation runs were made for methanol-steam and acetone-ethanol systems under total and partial condensation at atmospheric pressure, where total condensation means that the concentration of condensate is equal to that of vapor free stream. Ranges of variables for the present study were summarized in Table 1.

2. Experimental Results

2.1 Condensation heat transfer coefficients

Figure 2 shows a comparison of the observed

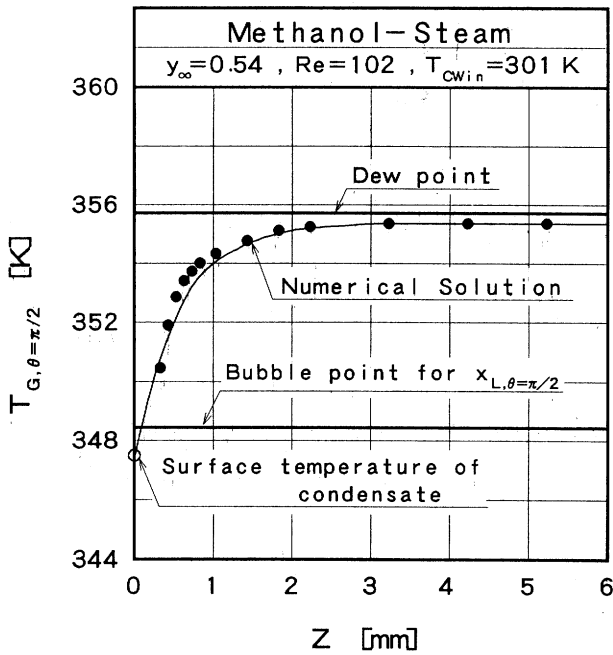


Fig. 3 An example of vapor phase temperature profile

condensation heat transfer coefficients with the theoretical ones by Nusselt's model under total condensation conditions, where concentrations of the condensate are equal to that of vapor, for concentrations of condensate of $x_L = 0.48 - 0.53$. The solid circles in the figure are condensation heat transfer coefficients defined by temperature driving forces between the surface temperatures of condensate and the wall temperatures ($T_{s, \theta = \pi/2} - T_w$). The open circles are the ones with temperature driving forces between vapor free stream temperatures and wall temperatures ($T_{\infty} - T_w$). The solid line in the figure is the theoretical value from Nusselt's model for nearly the same concentration of condensate ($x_L = 0.50$):

$$h_L = 0.725 \left(\frac{g \lambda_m \kappa_{Lm}^3 \rho_{Lm} (\rho_{Lm} - \rho_{G\infty})}{\mu_{Lm} (T_s - T_w) D} \right)^{1/4} \quad (4)$$

The condensation heat transfer coefficients with surface temperatures of the condensate showed good agreement with Nusselt's model within 10%, whereas the ones with vapor free stream temperatures showed much higher deviations.

2.2 Surface temperatures of condensate and vapor phase sensible heat fluxes

Figure 3 shows an example of the observed vapor phase temperature profiles on the equatorial plane of the condensing tube at $\theta = \pi/2$ for the methanol-steam system. The solid circles in the figure are the observed vapor phase temperatures and the open circle is the surface temperature of the condensate estimated by an extrapolation method. The solid line is the theoretical temperature profile for nearly the same operating conditions by numerical solution of the transport equations (Mamyoda and Asano, 1993) with the observed vapor free stream temperature, T_{∞} , and

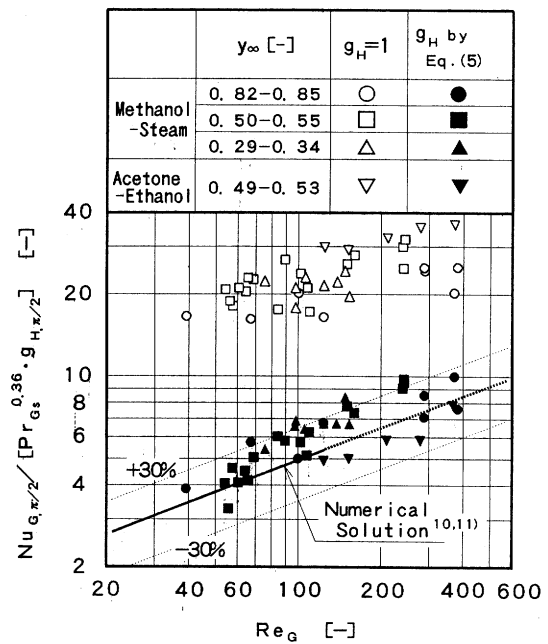


Fig. 4 Vapor phase sensible heat fluxes

extrapolated surface temperature of condensate, $T_{s, \theta = \pi/2}$. The two bold solid lines represent the dew point of the vapor and the bubble point of the condensate at $\theta = \pi/2$, where calculation of the latter value is described in the later discussions (Section 3.2).

Figure 4 shows the vapor phase local sensible heat fluxes at $\theta = \pi/2$, obtained from the observed vapor phase temperature profiles. The function g_H in the ordinate represents the effect of surface mass suction on the local sensible heat fluxes at $\theta = \pi/2$, of which value is calculated from our previous numerical correlation (Mamyoda and Asano, 1993, Mamyoda and Asano, 1994):

$$g_{H, \theta = \pi/2} = 1 / (a' + (1 - a') (1 + B_H)^{0.54}) \quad (5.a)$$

$$a' = -0.34 + 0.20Pr \quad (5.b)$$

The solid line in the figure represents correlation of the numerical solution at $\theta = \pi/2$ without surface mass suction (Mamyoda and Asano, 1993, Mamyoda and Asano, 1994):

$$Nu_{\theta = \pi/2, 0} = 0.82Re^{0.39} Pr^{0.36} \quad (6)$$

The solid keys are the observed vapor phase local sensible heat fluxes corrected for the effect of surface mass suction on the sensible heat fluxes by Eq. (5), and the open keys are the ones without correction for the effect of surface mass suction ($g_H = 1$). The observed vapor phase sensible heat fluxes corrected for the effect of surface mass suction agreed with the numerical correlation within 30%, whereas the ones without correction for the effect of surface mass suction showed much higher deviations.

2.3 Vapor phase mass and diffusion fluxes

Figure 5 shows the observed vapor phase average mass fluxes for the methanol-steam and the acetone-ethanol systems. The bold solid line in the figure represents the

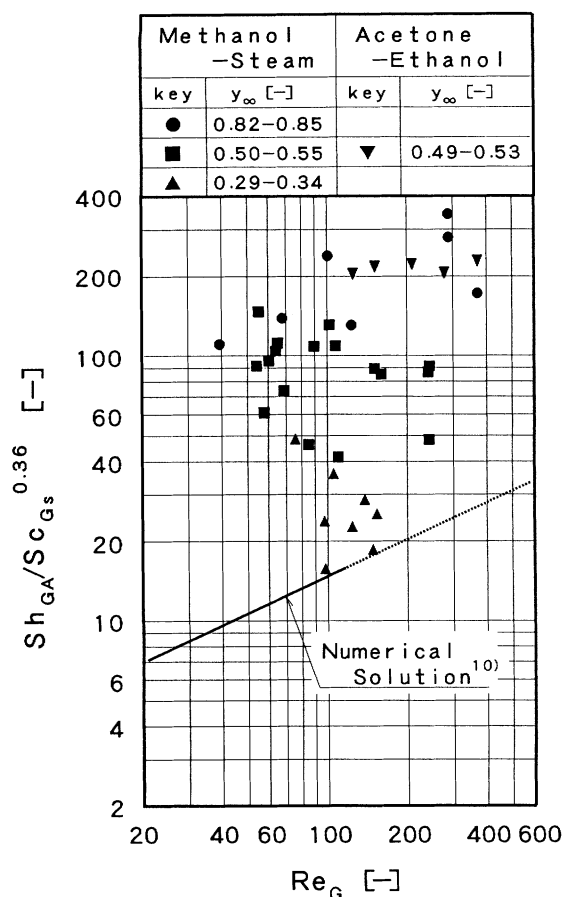


Fig. 5 Vapor phase mass fluxes

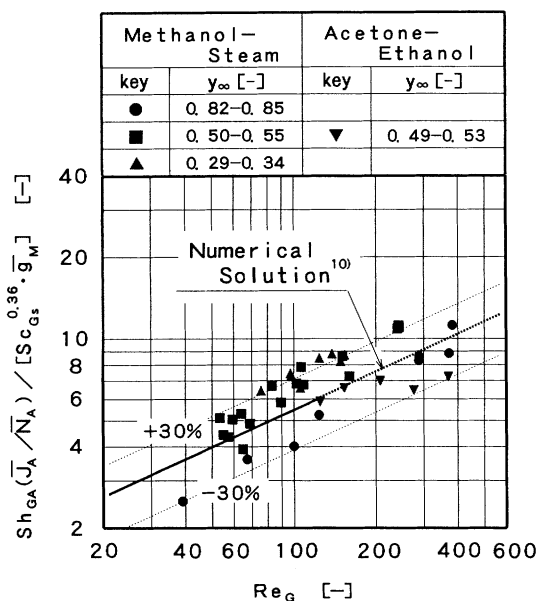


Fig. 6 Vapor phase diffusion fluxes

numerical correlation without surface mass suction (Mamyoda and Asano, 1993):

$$\{Sh(\bar{J}_A / \bar{N}_A)\}_0 = 0.66 Re^{0.46} Sc^{0.36} \quad (7)$$

The data showed much higher deviation from the numer-

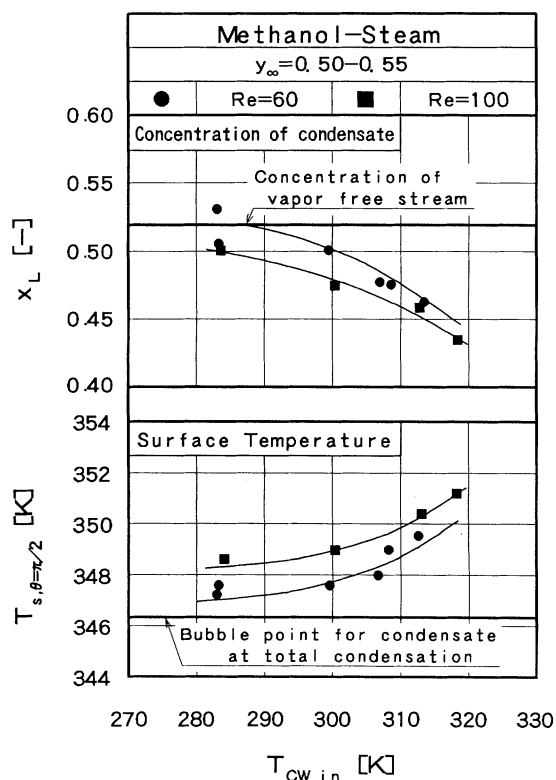


Fig. 7 Effect of vapor flow rate and cooling water temperature on concentration and surface temperature of condensate

ical correlation and irregular scattering. This may be due to the effect of convective mass flux, $(\bar{N}_A + \bar{N}_B) \omega_{As}$, shown in the second term of the right-hand side of Eq.(2).

Figure 6 shows the observed vapor phase average diffusion fluxes for the methanol-steam and the acetone-ethanol systems. The \bar{g}_M in the ordinate represents the numerical correlation for the effect of surface mass suction on the vapor phase average diffusion fluxes given by (Mamyoda and Asano, 1993):

$$\bar{g}_M = 1 / (a + (1-a)(1 + \bar{B}_M)^{0.67}) \quad (8.a)$$

$$a = 0.07 + 0.16 \log Sc \quad (8.b)$$

The diffusion fluxes corrected for surface mass suction agreed with numerical correlation within 30%, whereas no correlation was obtained for mass fluxes.

3. Discussion

3.1 Transition from total to partial condensation

Figure 7 shows the effect of cooling water temperatures on the concentrations and surface temperatures of the condensate with different vapor flow rates at $y_\infty = 0.51 - 0.54$. The bold solid line in the upper half of the figure is the free stream vapor concentration. The figure indicates the concentrations of the condensate increase with a decrease in cooling water temperature and approach that of total condensation. The observed surface temperatures of condensate at $\theta = \pi/2$, $T_{s, \theta = \pi/2}$, decrease with a decrease

Table 2 Basic equations for simulation

Vapor phase	
$\frac{Sh(J_A/N_A)_\theta}{Sh(J_A/N_A)_{\theta=0}} = (1 + a\theta^2 + b\theta^3) \bar{g}_M(Re, Sc, \bar{\phi})$	(9)
$\frac{Nu_\theta}{Nu_{\theta=0}} = (1 + a\theta^2 + b\theta^3) \bar{g}_H(Re, Pr, \bar{\phi})$	(10)
$Sh(J_A/N_A)_0 = f(Re, Sc)$	(11)
$Nu_0 = f(Re, Pr)$	(12)
$\bar{g}_M = 1 + 1.32\bar{\phi}^{1.05} Re^{0.54} Sc^{0.64}$	(13)
$\bar{g}_H = 1 + 1.32\bar{\phi}^{1.05} Re^{0.54} Pr^{0.64}$	(14)
$\bar{\phi} = \bar{v}_r / U_\infty$	(15)
Liquid phase	
$h_L = 0.725 \left(\frac{8\lambda_m K_{LM}^3 \rho_{LM} (\rho_{LM} - \rho_{G\infty})}{\mu_{LM} (T_s - T_w) D} \right)^{1/4}$	(4)
Interface	
$q_{L\theta} = \lambda_A N_{A\theta} + \lambda_B N_{B\theta} + q_{G\theta}$	(16)
Wall	
$q_{CW} = h_{CW} (T_w - T_{CW})$	(17)

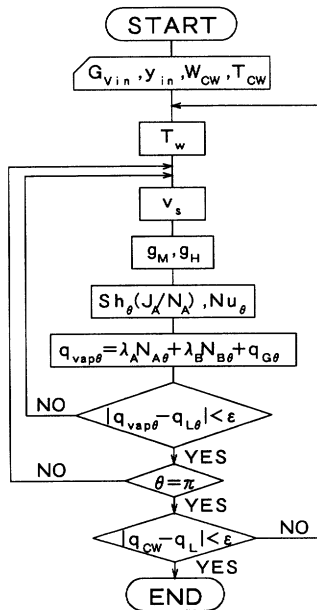


Fig. 8 Flow chart for simulation

in cooling water temperature and also approach to the bubble points of the condensate under total condensation. The figure also shows that transition from total to partial condensation is affected by vapor flow rates as well as cooling water temperature.

3.2 Simulation of condensation of binary vapor mixtures

The discussions in the previous sections can be applied for simulation of condensation of binary vapor mixtures on a short horizontal tube. The following are assumptions for the present simulation:

1. The vapor and condensate flows are laminar.

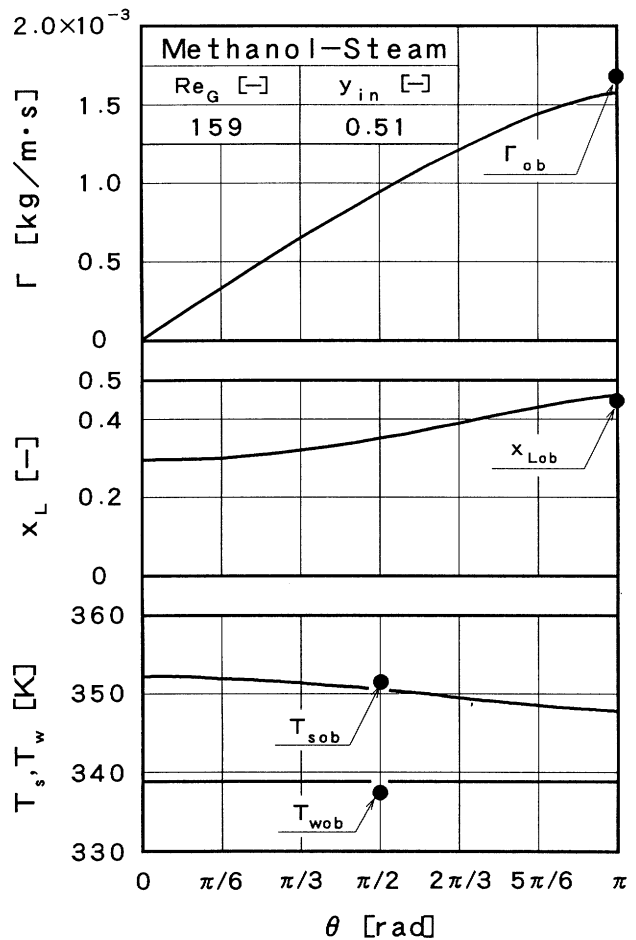


Fig. 9 Circumferential profiles of concentration, surface temperatures and flow rate of condensate

2. Nusselt's model is applicable to heat transfer through the condensate liquid film.

3. Numerical correlations for heat and mass transfer on a cylinder with surface mass suction are applied to estimation of vapor phase sensible heat and diffusion fluxes (Mamyoda and Asano, 1994).

4. Surface temperatures of the condensate are at their bubble point (Ito and Asano, 1982, Kosuge *et al.*, 1985).

5. Temperatures of the vapor free stream are at their dew point.

6. Wall temperature is uniform along the axial and circumferential direction.

The basic equations for the present simulation are summarized in **Table 2**. **Figure 8** shows a flow chart for the present simulation.

Figure 9 shows a comparison with the experimental data and present model, where variations in condensate flow rate, Γ , the concentration of the condensate, x_L , and the surface temperature of the condensate, T_s , in circumferential direction were shown together with observed ones. The calculation showed good agreement with observed data.

3.3 Prediction of the concentration of the condensate under partial condensation

Figure 10 shows a comparison of the surface

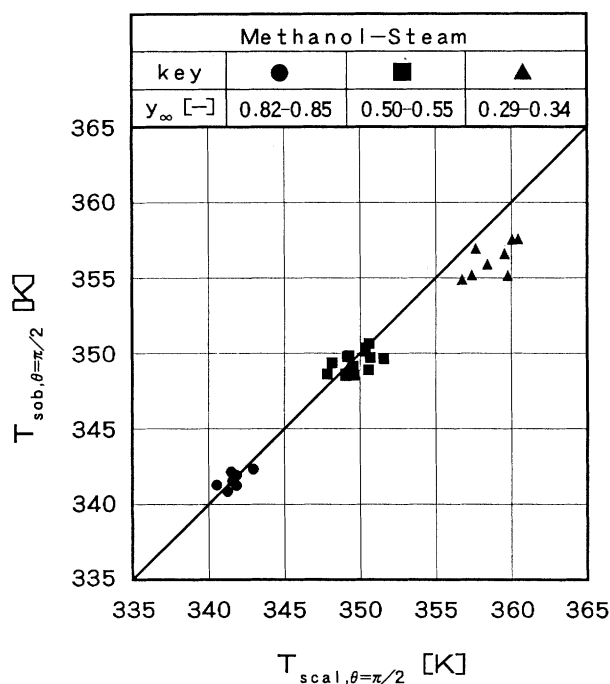


Fig. 10 Comparison between observed surface temperature of condensate and calculated one

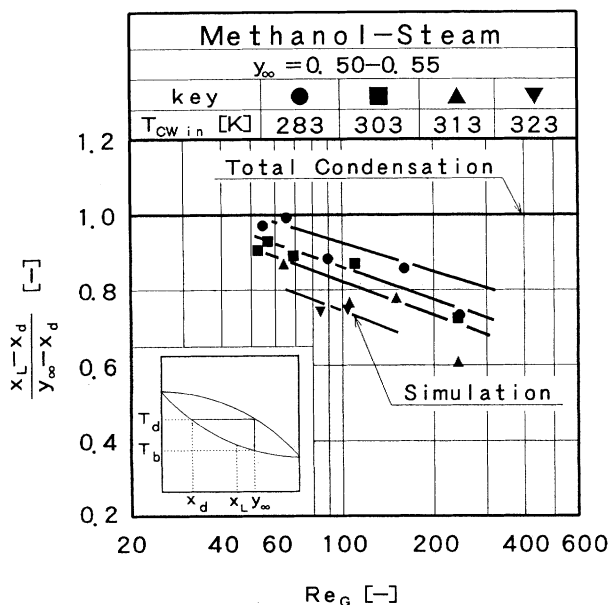


Fig. 11 Effect of vapor flow rate and cooling water temperature on partial condensation

temperatures at $\theta = \pi/2$ estimated by the present model (bubble point of the liquid at $\theta = \pi/2$, $T_{scal, \theta = \pi/2}$, with observed ones, $T_{sob, \theta = \pi/2}$, for total and partial condensation of binary vapor mixtures of the methanol-steam system. The observed data showed good agreement with calculated ones.

Figure 11 shows the variation of the liquid concentrations of the condensate with vapor phase Reynolds numbers and cooling water temperatures under total and partial condensation of binary vapor mixtures of the methanol-steam system. The ordinate of the figure repre-

sents degree of partial condensation, of which values vary from zero (without condensation) to unity (total condensation). The solid keys are observed values and solid lines are the predicted ones by the present model, which showed good agreement with the experimental data.

Conclusions

Measurements of the rates of condensation, the concentrations and the surface temperatures of the condensate, vapor phase sensible heat and diffusion fluxes were made for condensation of binary vapor mixtures on a short horizontal tube. The following conclusions were obtained.

1. Nusselt's model is applicable for heat transfer through condensate film based on the temperature driving forces between the surface temperatures of condensate and wall temperatures, $T_{s, \theta = \pi/2} - T_w$.
2. Observed vapor phase local sensible heat fluxes and average diffusion fluxes showed good agreement with the numerical correlation for heat and mass transfer on a cylinder with diffusive surface mass suction.
3. A new method for simulation of binary vapor mixtures on a short horizontal tube under total and partial condensation was proposed.

Nomenclature

- B_H = transfer number for heat transfer
($= Re \cdot Pr \cdot \phi / Nu$) [-]
- B_M = transfer number for mass transfer
($= Re \cdot Sc \cdot \phi / Sh (J_A / N_A)$) [-]
- c_p = specific heat at constant pressure [J/(kg·K)]
- \mathcal{D} = binary diffusion coefficient [m^2/s]
- D = diameter of condensing tube [m]
- g = acceleration of gravity [m/s^2]
- g_H = function of high mass flux effect for heat transfer [-]
- g_M = function of high mass flux effect for mass transfer [-]
- G_V = vapor mass flow rate [kg/s]
- h_{cW} = heat transfer coefficient of cooling water [$W/(m^2 \cdot K)$]
- h_L = condensation heat transfer coefficient [$W/(m^2 \cdot K)$]
- J_A = diffusion flux of more volatile component [$kg/(m^2 \cdot s)$]
- N_A = mass flux of more volatile component [$kg/(m^2 \cdot s)$]
- Nu = Nusselt number ($= q_G D / \kappa (T_\infty - T_s)$) [-]
- Pr = Prandtl number ($= c_p \mu / \kappa$) [-]
- q_G = sensible heat flux for vapor phase [W/m^2]
- q_L = latent heat flux of condensation of vapor [W/m^2]
- q_{vap} = sum of sensible and latent heat flux for vapor phase [W/m^2]
- r = radial distance from center of condensing tube [m]
- Re = Reynolds number ($= \rho_\infty U_\infty D / \mu_\infty$) [-]
- Sc = Schmidt number ($= \mu / \rho \mathcal{D}$) [-]
- Sh = Sherwood number ($= N_A D / \rho_s \mathcal{D}_s (\omega_\infty - \omega_s)$) [-]
- T = temperature [K]
- T_b = bubble point of liquid [K]
- T_d = dew point of vapor [K]
- T_{ref} = reference temperature ($= T_w + (T_s - T_w)/3$) [K]
- U_∞ = free stream velocity [m/s]
- v_r = radial component of suction velocity at the surface of the condensate [m/s]
- x = mole fraction of liquid [-]
- y = mole fraction of vapor [-]
- Γ = condensate flow rate [kg/(m·s)]
- θ = angle from front stagnation point [rad]

κ	= thermal conductivity	[W/(m·K)]
λ	= latent heat of vaporization	[J/kg]
μ	= viscosity	[Pa·s]
ρ	= density	[kg/m ³]
ϕ	= suction ratio at the surface of the condensate ($=v_s/U_\infty$)	[-]
ω	= mass fraction of more volatile component	[-]

<Subscript>

A	= more volatile component
B	= less volatile component
CW	= cooling water
G	= vapor phase
in	= inlet vapor
L	= liquid phase (condensate)
m	= mixture
s	= surface of the condensate
w	= wall
θ	= local value at angle θ
∞	= free stream
0	= without surface mass suction or injection

<Superscript>

-	= average value
---	-----------------

Literature Cited

- Asano, K. and S. Matsuda; "Total and Partial Condensation of Binary Vapor Mixtures of Methanol/Water Systems on a Vertical Flat Plate," *Kagaku Kogaku Ronbunshu*, **11**, 27-33 (1985)
- Bandrowski, J. and A. Bryczkowski; "Experimental Study of Heat Transfer at the Total Condensation of Mixed Vapours of Miscible Liquids," *Int. J. Heat Mass Transfer*, **18**, 503-512 (1975)
- Colburn, A.P. and T.B. Drew; "The Condensation of Mixed Vapors," *Trans. AIChE*, **33**, 197-215 (1937)
- Denny, V.E. and V.J. Jusionis; "Effects of Forced Flow and Variable Properties on Binary Film Condensation," *Int. J. Heat Mass Transfer*, **15**, 2143-2153 (1972)
- Fujii, T. and S. Koyama; "Laminar Forced Convective Condensation of a Ternary Vapor Mixture on a Flat Plate," *ASME-HTD*, **38**, Fundamentals of Phase Change, 81-87 (1985)
- Fujii, T., S. Koyama and M. Watabe; "Laminar Film Condensation of Gravity-Controlled Convection for Ternary Vapor Mixtures on a Vertical Flat Plate," *Nippon Kikai Gakkai Ronbunshu*, **B-510**, 434-441 (1989)
- Ito, A. and K. Asano; "Thermal Effects in Non-Adiabatic Binary Distillation - Effects of Partial Condensation of Mixed Vapors on the Rates of Heat and Mass Transfer and Prediction of H.T.U.," *Chem. Eng. Sci.*, **37**, 1007-1014 (1982)
- Kirkbride, C.G.; "Heat Transmission by Condensing Pure and Mixed Substances on Horizontal Tubes," *Ind. Eng. Chem.*, **25**, 1324-1330 (1933)
- Kosuge, H., T. Johkoh and K. Asano; "Experimental Studies of Diffusion fluxes of Ternary Distillation of the Acetone-Methanol-Ethanol Systems by a Wetted-Wall Column," *Chem. Eng. Commun.*, **34**, 111-122 (1985)
- Mamyoda, T. and K. Asano; "Numerical Analysis of Drag Coefficients and Heat and Mass Transfer of a Cylinder with Diffusive Surface Mass Suction or Injection," *J. Chem. Eng. Japan*, **26**, 382-388 (1993)
- Mamyoda, T. and K. Asano; "Experimental Study of Condensation of Vapors in the Presence of Noncondensable Gas on a Short Horizontal Tube," *J. Chem. Eng. Japan*, **27**, 485-491 (1994)
- Minkowycz, W.J. and E.M. Sparrow; "Condensation Heat Transfer in the Presence of Noncondensables, Interfacial Resistance, Superheating, Variable Properties and Diffusion," *Int. J. Heat Mass Transfer*, **9**, 1125-1144 (1966)
- Pressburg, B.S. and J.B. Todd; "Heat Transfer Coefficients for Condensing Organic Vapors of Pure Components and Binary Mixtures," *AIChE J.*, **3**, 348-352 (1957)
- Sykes, J.A. and J.M. Marchello; "Condensation of Immiscible Liquids on Horizontal Tube," *Ind. Eng. Chem. Process Des. Develop.*, **9**, 63-71 (1970)